

## Supporting Information for

### Structural Characterisation and Elucidation of the Electronic Structure of the Mononuclear Pt(III) Complex $[\text{Pt}(\text{[9]aneS}_3)_2]^{3+}$ ( $\text{[9]aneS}_3 = 1,4,7\text{-trithiacyclononane}$ )

Emma Stephen, Alexander J. Blake, E. Stephen Davies, Jonathan McMaster\* and Martin Schröder\*

*School of Chemistry, University of Nottingham, Nottingham NG7 2RD, UK.*

#### Preparation of $[\text{Pt}(\text{[9]aneS}_3)_2](\text{PF}_6)_2$ (1)

PtCl<sub>2</sub> (96 mg, 0.36 mmol) was reacted with [9]aneS<sub>3</sub> (140 mg, 0.78 mmol) in H<sub>2</sub>O and MeOH (1:1 V, 20 mL) by heating to reflux for 1 h. To the resulting orange solution, NH<sub>4</sub>PF<sub>6</sub> was added in excess and the solution cooled to precipitate an orange-yellow solid. The solid was collected and dissolved in CH<sub>3</sub>CN and diffused with Et<sub>2</sub>O to yield  $[\text{Pt}(\text{[9]aneS}_3)_2](\text{PF}_6)_2$  as orange crystals. Yield 171 mg, 56%. Found: C, 16.93; H, 2.84. Calc. for C<sub>12</sub>H<sub>24</sub>S<sub>6</sub>P<sub>2</sub>F<sub>12</sub>Pt: C, 17.04; H, 2.86 IR (KBr)  $\nu/\text{cm}^{-1}$ : 3432 (w), 2990 (w), 1635 (vw), 1443 (w), 1413 (m), 1306 (w), 1289 (w), 1156 (w), 1090 (w), 1005 (vw), 835 (vs, broad), 741 (m), 651 (w), 557 (vs). M.S. (ES): *m/z* 555 for  $[\text{Pt}(\text{[9]aneS}_3)_2]^{2+}$  with correct isotopic distribution. UV/vis  $\lambda_{\text{max}}$  (CH<sub>3</sub>CN)/nm 436 ( $\epsilon_{\text{max}}/\text{L mol}^{-1} \text{ cm}^{-1}$  101.4, broad).

#### X-ray single crystal structure determination of $[\text{Pt}(\text{[9]aneS}_3)_2](\text{PF}_6)_2 \cdot 2\text{CH}_3\text{CN}$ (1.2MeCN)

An orange block crystal ( $0.42 \times 0.39 \times 0.21 \text{ mm}^3$ ) was coated with Fomblin perfluoropolyether (YR-1800; Lancaster Synthesis) and mounted on a glass fiber for data collection using the Bruker SMART 1000 CCD area detector in Nottingham. The wavelength used was 0.71073 Å.

**Crystal data.** Crystal data: C<sub>12</sub>H<sub>24</sub>S<sub>6</sub>P<sub>2</sub>F<sub>12</sub>Pt.CH<sub>3</sub>CN,  $M = 927.81$ , Orthorhombic,  $a = 11.9244(8)$ ,  $b = 21.6165(14)$ ,  $c = 11.3781(7)$  Å,  $V = 2932.9(6)$  Å<sup>3</sup>,  $T = 150(2)$  K, space group *Pccn*,  $Z = 4$ ,  $D_c = 2.101 \text{ g/cm}^3$ , 3800 unique reflections ( $R_{\text{int}} = 0.025$ ).

The structure was solved by direct methods using the SHELXTL program package<sup>1</sup> and all non-hydrogen atoms were refined with anisotropic displacement parameters. When refined using an ordered model, the equatorial F atoms of both PF<sub>6</sub><sup>-</sup> anions developed highly prolate ellipsoids. Attempts to model this disorder in terms of up to four atomic sites per F were unsuccessful, and the most satisfactory refinement was achieved by reverting to a model with one atomic site per F atom and allowing extreme ellipsoids to encompass multiple orientations. Application of similarity restraints to the P-F distances led to stable refinement and convergence.

Final  $R_1[F > 2\sigma(F)] = 0.0287$ ,  $wR_2$  (all data) = 0.0651.

Bond lengths and angles for  $[\text{Pt}(\text{[9]aneS}_3)_2]^{2+}$  in 1.2MeCN are given in Tables S1 and S2, respectively and a view of the  $[\text{Pt}(\text{[9]aneS}_3)_2]^{2+}$  cation in 1.2MeCN is shown in Fig. S1.

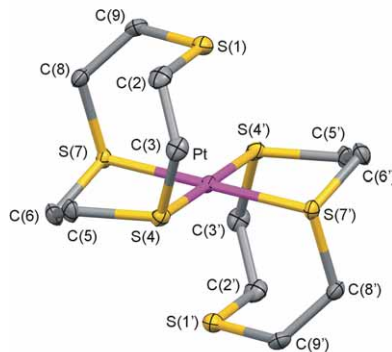


**Figure S1.** A view of the  $[\text{Pt}([\text{9}] \text{aneS}_3)_2]^{2+}$  cation in 1.2MeCN; displacement ellipsoids are drawn at the 50% probability level and hydrogen atoms are omitted for clarity.

#### Electrochemical generation of $[\text{Pt}([\text{9}] \text{aneS}_3)_2](\text{PF}_6)_3$ (2)

Cyclic voltammetric (Fig. S2) and coulometric studies were carried out using an Autolab PGSTAT20 potentiostat. Cyclic voltammetry was carried out under an Ar atmosphere using a three-electrode arrangement in a single compartment cell. A glassy carbon working electrode, a Pt wire secondary electrode and a saturated calomel reference electrode, chemically isolated from the test solution *via* a bridge tube containing electrolyte solution and fitted with a porous vycor frit, were used in the cell. Bulk electrolysis experiments at a controlled potential were carried out using a two-compartment cell. The Pt/Rh gauze basket working electrode was separated from the wound Pt/Rh gauze secondary electrode by a glass frit. A saturated calomel reference electrode was bridged to the test solution through a vycor frit orientated at the centre of the working electrode. The working electrode compartment was fitted with a magnetic stirrer bar and the test solution was stirred rapidly during electrolysis. The Pt(II) complex  $[\text{Pt}([\text{9}] \text{aneS}_3)_2](\text{PF}_6)_2$  (11.8 mg,  $13.9 \times 10^{-3}$  mmol) in  $\text{CH}_3\text{CN}$  (7 mL) containing  $\text{NBu}_4\text{PF}_6$  (0.1 M) was oxidized at +0.6V *vs.*  $\text{Fc}^+/\text{Fc}$  at 273 K under an Ar atmosphere. The resultant intense yellow solution was transferred from the cell via cannula into an Ar purged Schlenk flask. Dark yellow plate crystals suitable for X-ray crystallographic analysis were obtained by vapor diffusion of  $\text{Et}_2\text{O}$  into the solution. UV-vis (in  $\text{CH}_3\text{CN}$ ) [ $\lambda_{\text{max}}(\varepsilon_{\text{max}})$ ]: 396 nm ( $5700 \text{ M}^{-1} \text{ cm}^{-1}$ , broad).

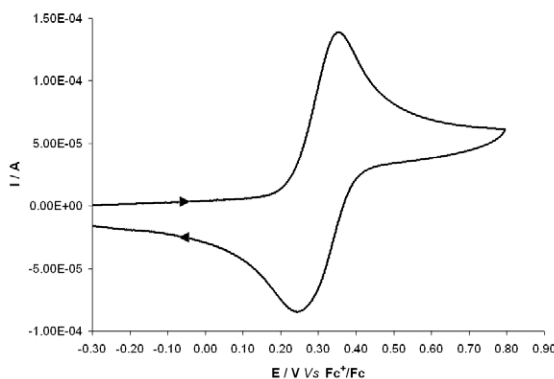


**Figure S2:** Cyclic voltammogram of  $[\text{Pt}([\text{9}] \text{aneS}_3)_2](\text{PF}_6)_2$  in MeCN containing  $\text{NBu}_4\text{PF}_6$  (0.2 M) at 298 K at a scan rate of 100  $\text{mVs}^{-1}$ .

The UV/vis spectroelectrochemical experiments (Fig. S3) were carried out using an optically transparent electrochemical (OTE) cell (modified quartz cuvette, optical pathlength: 0.5 mm). A three-electrode configuration, consisting a Pt/Rh gauze working electrode, a Pt wire secondary electrode (in a fritted PTFE sleeve) and a saturated calomel electrode, chemically isolated from the test solution *via* bridge tube containing electrolyte solution and terminated in a porous frit, was used in the cell. The potential at the working electrode was controlled by a Sycopel Scientific Ltd. DD10M potentiostat. The UV/vis spectra were recorded on a Perkin Elmer Lambda 16 spectrophotometer. The cavity was purged with N<sub>2</sub> and temperature control at the sample was achieved by flowing cooled N<sub>2</sub> across the surface of the cell.

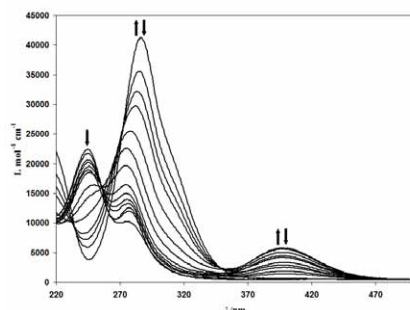


**Figure S3:** In situ UV/vis absorption spectra of  $[\text{Pt}([\text{9}] \text{aneS}_3)_2](\text{PF}_6)_2$  in MeCN (0.2 M NBu<sub>4</sub>PF<sub>6</sub>, 243K) at +0.69 V (vs. Fc<sup>+</sup>/Fc)

#### X-ray single crystal structure determination of $[\text{Pt}([\text{9}] \text{aneS}_3)_2](\text{PF}_6)_3 \cdot \text{CH}_3\text{CN}$ (2.MeCN)

A dark yellow plate crystal ( $0.26 \times 0.23 \times 0.03 \text{ mm}^3$ ) was coated with frozen Fomblin perfluoropolyether (YR-1800; Lancaster Synthesis) and mounted on a glass fiber for data collection using the Bruker SMART APEX diffractometer in Nottingham. The wavelength used was 0.71073 Å.

**Crystal data.** Crystal data: C<sub>12</sub>H<sub>24</sub>S<sub>6</sub>P<sub>3</sub>F<sub>18</sub>Pt.CH<sub>3</sub>CN,  $M = 1031.73$ , Orthorhombic,  $a = 9.2153(5)$ ,  $b = 17.3138(9)$ ,  $c = 18.8681(10)$  Å,  $V = 3010.4(5)$  Å<sup>3</sup>,  $T = 150(2)$  K, space group  $P2_12_12_1$ ,  $Z = 4$ ,  $D_c = 2.276$  g/cm<sup>3</sup>, 6823 unique reflections ( $R_{\text{int}} = 0.038$ ).

The structure was solved by direct methods using the SHELXTL program package<sup>1</sup> and all non-hydrogen atoms were refined with anisotropic displacement parameters. When refined using an ordered model, the equatorial F atoms of one PF<sub>6</sub><sup>-</sup> anion developed extreme anisotropic displacement parameters. Examination of difference maps indicated that each equatorial F atom was disordered over three sites. A successful refinement was achieved by using extensive distance and angle restraints; the equatorial F atom components were restrained to be coplanar with each other and with the central P' atom; finally, the occupancies for the three disorder components were refined subject to the restraint that they summed to unity. The final refined occupancies for the three disorder components were 0.38(2), 0.43(2) and 0.188(11). Isotropic displacement parameters for all equatorial F atom components refined freely to acceptable values, and each disorder component exhibited sensible geometry. Application of disorder modeling with distance and angle restraints to one PF<sub>6</sub><sup>-</sup> anion led to stable refinement. Final  $R_1[F > 2\sigma(F)] = 0.0325$ ,  $wR_2$  (all data) = 0.0780.

Bond lengths and angles for  $[\text{Pt}([\text{9}] \text{aneS}_3)_2]^{3+}$  in 2.MeCN are given in Tables S1 and S2, respectively.

	<b>1.2MeCN</b>	<b>2.MeCN</b>	DFT Calculated
Pt-S(1)	3.0570(11)	2.5832(14)	2.687
Pt-S(4)	2.2925(10)	2.3467(15)	2.403
Pt-S(7)	2.2995(10)	2.3423(13)	2.400
Pt-S(1)	3.0570(11)	2.5762(13)	2.689
Pt-S(4')	2.2925(10)	2.3445(14)	2.399
Pt-S(7')	2.2995(10)	2.3442(14)	2.399

**Table S1** Bond lengths (/ $\text{\AA}$ ) for  $[\text{Pt}([9]\text{aneS}_3)_2]^{2+}$  in **1.2MeCN**,  $[\text{Pt}([9]\text{aneS}_3)_2]^{3+}$  in **2.MeCN** and  $[\text{Pt}([9]\text{aneS}_3)_2]^{3+}$  calculated by DFT.

	<b>1.2MeCN</b>	<b>2.MeCN</b>	DFT Calculated		<b>1.2MeCN</b>	<b>2.MeCN</b>	DFT Calculated
S7-Pt-S7'	180.00	178.70(5)	179.4	S4'-Pt-S1'	84.90(3)	87.80(5)	86.1
S7-Pt-S4'	90.80(4)	90.72(5)	91.9	S4-Pt-S1'	95.11(3)	91.08(5)	93.5
S7'-Pt-S4'	89.20(4)	89.33(5)	88.0	S7-Pt-S1	83.48(3)	87.88(5)	85.2
S7-Pt-S4	89.20(4)	89.22(5)	88.1	S7'-Pt-S1	96.52(3)	93.41(5)	95.4
S7'-Pt-S4	90.80(4)	90.70(6)	92.0	S4'-Pt-S1	95.11(3)	94.04(5)	94.5
S4'-Pt-S4	180.00	178.88(6)	179.6	S4-Pt-S1	84.90(3)	87.08(5)	85.9
S7-Pt-S1'	96.52(3)	90.59(5)	94.0	S1'-Pt-S1	180.00	177.62(6)	179.1
S7'-Pt-S1'	83.48(3)	88.12(5)	85.4				

**Table S2** Bond angles ( $^{\circ}$ ) for  $[\text{Pt}([9]\text{aneS}_3)_2]^{2+}$  in **1.2MeCN**  $[\text{Pt}([9]\text{aneS}_3)_2]^{3+}$  in **2.MeCN** and  $[\text{Pt}([9]\text{aneS}_3)_2]^{3+}$  calculated by DFT.

#### Crystallographic data:

**1.2MeCN:**  $[\text{Pt}([9]\text{aneS}_3)_2](\text{PF}_6)_2 \cdot 2\text{CH}_3\text{CN}$ , orthorhombic,  $Pccn$ ,  $a = 11.9244(8)$ ,  $b = 21.6165(14)$ ,  $c = 11.3781(7)$   $\text{\AA}$ ,  $V = 2932.9(6)$   $\text{\AA}^3$ ,  $Z = 4$ ,  $D_c = 2.101$  g  $\text{cm}^{-3}$ ,  $T = 150(2)$  K,  $\lambda = 0.71073$   $\text{\AA}$ ; 3800 independent reflections observed [R(int) = 0.025], which were used in all calculations. Final  $R_1$  [ $F > 4\sigma(F)$ ] = 0.0287,  $wR_2$  (all data) = 0.0651.

**2.MeCN:**  $[\text{Pt}([9]\text{aneS}_3)_2](\text{PF}_6)_3 \cdot \text{CH}_3\text{CN}$ , orthorhombic,  $P2_12_12_1$ ,  $a = 9.2153(5)$ ,  $b = 17.3138(9)$ ,  $c = 18.8681(10)$   $\text{\AA}$ ,  $V = 3010.4(5)$   $\text{\AA}^3$ ,  $Z = 4$ ,  $D_c = 2.276$  g  $\text{cm}^{-3}$ ,  $T = 150(2)$  K,  $\lambda = 0.71073$   $\text{\AA}$ ; 6823 independent reflections observed [R(int) = 0.038], which were used in all calculations.  $R_1$  [ $F > 4\sigma(F)$ ] = 0.0325,  $wR_2$  (all data) = 0.0780; the final value of the Flack parameter is 0.012(5).

### EPR Spectroscopy and Simulation

The X-band fluid and frozen EPR spectra of  $[\text{Pt}(\text{[9]aneS}_3)_2]^{3+}$  were recorded on a Bruker EMX EPR spectrometer. The spectrum of the fluid solution (Fig. S4) was recorded at ambient temperatures and the frozen solution spectrum recorded at *ca.* 77 K using a finger dewar filled with liquid N<sub>2</sub>. The simulation of the EPR spectra for the Pt(III) complex in a frozen solution was performed using the Easyspin package version 2.7.0.<sup>2</sup>

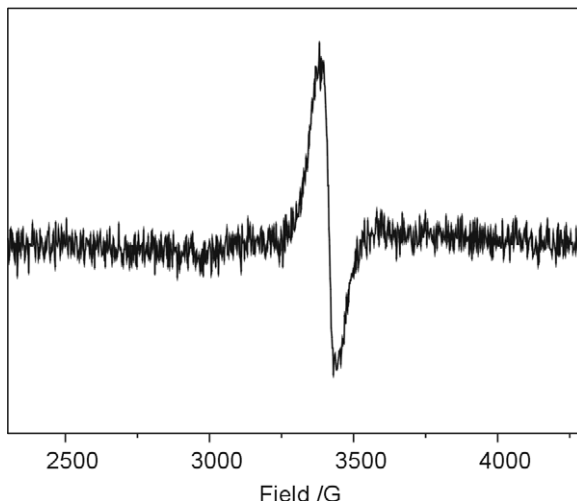


**Figure S4** X-band EPR fluid solution spectrum of  $[\text{Pt}(\text{[9]aneS}_3)_2]^{3+}$  at room temeprature in HClO<sub>4</sub>.

### DFT Calculations on $[\text{Pt}(\text{[9]aneS}_3)_2]^{3+}$

The calculations were performed using the Amsterdam Density Functional (ADF) suite version 2005.01.<sup>3,4</sup> The unrestricted scalar relativistic DFT calculations employed a Slater type orbital (STO) triple- $\zeta$ -plus one polarization function basis set from the ZORA/TZP database of the ADF suite for all atoms. The cores were frozen up to and including 2p for S, 1s for C and 4d for Pt respectively. The local density approximation (LDA) with the correlation potential due to Vosko *et al*<sup>5</sup> was used in all of the DFT calculations. Gradient corrections were performed using the functionals of Becke<sup>6</sup> and Perdew (BP).<sup>7</sup> A model of  $[\text{Pt}(\text{[9]aneS}_3)_2]^{3+}$  was constructed using geometrical data from the X-ray crystal structure and were optimized without any constraints on symmetry. The co-ordinate frame used in the calculations places the x-axis along the bisector of the S(4')-Pt-S(7') bond angle, the y-axis in the PtS<sub>4</sub> equatorial plane and the z-axis perpendicular to the PtS<sub>4</sub> equatorial plane.

### Geometry Optimized Coordinates for $[\text{Pt}(\text{[9]aneS}_3)_2]^{3+}$

Pt	0.00000	0.00000	0.00000
H	2.92077	0.60727	1.76892
H	4.04291	1.29413	0.57870
H	4.02041	-1.29689	0.62931
C	3.13974	0.67508	0.69427
H	-1.54980	1.73489	3.80022
H	-1.60556	-1.70197	3.78664
S	-0.32121	0.00915	2.66781

C	3.31926	-0.68185	0.04491
H	-0.35578	-2.35203	2.71813
C	-1.17761	-1.62486	2.77525
C	-1.70797	1.23465	2.83330
H	3.70089	-0.61512	-0.98115
H	-0.84353	2.94624	1.77019
S	1.72479	1.66673	0.01238
H	-2.65220	0.68202	2.90229
S	1.72591	-1.66673	-0.01238
C	-1.72596	2.29183	1.73641
H	-2.61249	2.93815	1.82813
H	3.11462	1.28055	-1.94831
H	2.53920	2.95623	-1.83656
C	-2.26512	-1.89409	1.74621
H	-2.58085	-2.94646	1.80768
C	2.22926	1.90243	-1.77435
H	-3.15206	-1.26806	1.89981
H	2.57454	-2.93667	-1.86944
C	1.69185	-2.28720	-1.76107
H	2.60328	-0.67915	-2.94434
S	-1.72710	1.67016	-0.01238
H	0.80730	-2.93860	-1.78052
S	-1.72499	-1.66816	-0.02990
H	-3.72519	0.61809	0.90897
C	1.65924	-1.23100	-2.85909
C	1.12385	1.63414	-2.78330
H	0.29784	2.35564	-2.70426
C	-3.31737	0.68322	-0.10590
H	1.53093	1.72358	-3.80259
S	0.27749	-0.00460	-2.67421
H	1.48588	-1.73244	-3.82306
C	-3.12014	-0.67482	-0.74987
H	-4.00313	1.29565	-0.71034
H	-4.02699	-1.29276	-0.66027
H	-2.86999	-0.60721	-1.81720

Energy: -7.130659490773601 Hartree

## References

1. G. M. Sheldrick, *Acta Crystallogr., Sect. A* 2008, **64**, 112-122.
2. S. Stoll and A. Schweiger, *J. Magn. Reson.* 2006, **178**, 42-55; S. Stoll and A. Schweiger, *Biol. Magn. Reson.* 2007, **27**, 299-321.
3. C. Fonseca Guerra, J. G. Snijders, G. te Velde and E. J. Baerends, *E. J. Theor. Chem. Acc.* 1998, **99**, 391-403.
4. G. te Velde, F. M. Bickelhaupt, S. J. A. van Gisbergen, C. Fonseca Guerra, E. J. Baerends, J. G. Snijders and T. Ziegler, *J. Comput. Chem.* 2001, **22**, 931-967.
5. S. H. Vosko, L. Wilk and M. Nusair, *M. Can. J. Phys.* 1980, **58**, 1200-1211.
6. A. D. Becke, *Phys. Rev. A.* 1988, **38**, 3098-3100.
7. J. P. Perdew, *Phys. Rev. B.* 1986, **33**, 8822-8824.